

This paper is similar in contents to the one with the same title published in Industrial and Engineering Chemistry Research, 34 (8) 2769 - 2781, 1995.

Waves in a Two-Component System: The Oxide Surface as a Variable Charge Adsorbent

Joachim Gruber

(jochen.gruber@acamedia.info)

Address at the time this paper was published:

Arbeitsbereich Umweltschutztechnik, TU Harburg

Eißendorfer Straße 40, D 21073 Hamburg

Abstract

Concentration waves, the solutions of the Riemann problem, are calculated in the framework of multicomponent chromatography. Unlike ion exchange surfaces, oxides bind cations by predominantly chemical forces, except perhaps in pristine water (at low ionic strengths $I \leq 10^{-4}$ mol/L and trace metal concentrations), where electrostatic constraints give adsorption the appearance of a metal-proton exchange process. In addition to the ionic strength threshold there is another threshold in concentration space, a line along which the metal ions cover half of the surface sites (equivalence line). On its low pH side analytical expressions for the waves in pristine water are good approximations for the $I = 0.1$ mol/L case, as constructed from eigenvectors and eigenvalues of the Jacobian of the multicomponent isotherms. At pH above the equivalence threshold competition for adsorption sites has a negligible effect on the waves in water at $I = 0.1$ mol/L.

In the past decade affordable computers have become capable of calculating geochemical transport of several interacting chemical components in porous media. Examples of such components are natural ions, ligands, nutrients and contaminants. Numerous transport codes have been written, as is evident from reviews e.g. by Kirkner and Reeves (1, 2) or Kinzelbach et al. (3). Numerical difficulties and long computation times have been addressed in various ways, depending on the choice of the geochemical problem (4 - 9).

The analytical solution of the transport equation for the system with one adsorbing component, no soluble complex formation and no precipitation (10) shows that, once a stable concentration profile has developed, its form does not tell us whether it has been generated by hydrodynamic dispersion or by kinetics of adsorption with a linear driving force. In fact, for a water velocity of 1 m/yr or less - typical for sandy/loamy soils- the kinetics of adsorption disappears behind hydrodynamic dispersion when the time constant for adsorption is a week or less. This will also be assumed in this paper although an analytical solution of the general multicomponent transport equations has not been found.

At thermodynamic equilibrium chemical interactions are described by mass action laws, which are nonlinear in the soluble concentrations of the components. Because of this nonlinearity the system behavior is characterized by a multitude of thresholds. The presence of a component is largely irrelevant when its concentration stays below a threshold. When its concentration increases and crosses the threshold, it may gain more influence than any of the other components has.

These thresholds in concentration space are well known in batch systems where they delimit regions of predominance of a species (11). Concentration space is the space the coordinate axes of which are the concentrations of the chemical components. The locations of thresholds in concentration space are similarly necessary to help us understand transport profiles in columns.

The following is true both for nonlinear batch and transport systems:

(1) The behavior of a system, as expressed by its speciation or its concentration profile, changes qualitatively across a threshold. We need to know the thresholds before we can draw conclusions based on a limited number of samples of the system behavior. Such conclusions are inter-, extrapolation and generalization of computed or experimentally determined results.

(2) Form and location of the thresholds in concentration space are functions of the chemical interaction parameters, e.g. complex formation constants, selectivity coefficients or solubility products. The thresholds cannot be located applying a numerical solution technique to the complete multicomponent chemical system, sampling the behavior at more or less arbitrarily chosen locations in concentration space. Instead, analytical solutions have to be found for simplified versions of the system with which to make informed guesses of the governing processes and thus of the expected location of the thresholds.

One such simplification of the 1-dimensional multicomponent transport problem is omitting diffusion and hydrodynamic dispersion, thus reducing the transport equations to a nonlinear set of hyperbolic partial differential equations in one space coordinate and time as used in multicomponent chromatography (13, 14). The concentration profile is then usually more easily computed than with numerical models, largely because general properties of the solution of the hyperbolic problem can be derived from mathematics and do not need to be found by the computer (12, 15 - 17).

In chromatography any concentration profile can be built from interacting centered waves originating from the concentration inhomogeneities within the column (12, 13, 18). The centered wave is the solution of the transport equations for the so-called "Riemann Problem", i.e. a single abrupt change of the chemical composition of the water (feed) at the inlet of a column with a homogeneous concentration distribution.

Whereas ion exchange resins interact with ions via electrostatic forces, the adsorbing surfaces considered in this paper -ferric oxides- bind ions by predominantly chemical forces. Thus the surface generally acquires electric charge as more and more ions adsorb. Mainly because of the absence of data and appropriate chemical models, this paper will limit itself to systems where two components, a metal ion and the proton, compete for adsorption sites. We will derive the concentration profile of the centered wave from the chemical interactions.

In some areas of concentration space the structure of the solution is indicative of accumulation of one component after remobilization due to

competition of the other (displacement development). The thresholds leading into those areas will be located

Governing Hyperbolic Equations

Migration of two chemical components, a metal M and the proton H, in homogeneous porous media or a flow channel of a non homogeneous medium is described by two mass conservation laws. In the absence of hydrodynamic dispersion, precipitation and dissolution of solids and when the pore water is in thermodynamic equilibrium with the adsorbing surfaces, the conservation laws are hyperbolic equations that are nonlinear due to the adsorption isotherms $\underline{M}(M, H)$ and $\underline{H}(M, H)$:

$$\frac{\partial}{\partial t} \{ \phi M(x,t) + \underline{M}(M, H) \} + q \frac{\partial}{\partial x} M(x,t) = 0 \quad (1)$$

$$\frac{\partial}{\partial t} \{ \phi H_t(x,t) + \underline{H}(M, H) \} + q \frac{\partial}{\partial x} H_t(x,t) = 0 \quad (2)$$

Here x and t are the space and time coordinates, ϕ and q are the volumetric water content of the porous medium and the flux of the water, respectively. $M(x, t)$, $\underline{M}(M, H)$ and $H_t(x, t)$, $\underline{H}(M, H)$ are the soluble and adsorbed metal and proton concentrations, respectively. It is assumed that the only soluble species of the metal is the free metal ion, M^{2+} , and that there are several soluble proton species, the concentration of which add up to $H_t(x, t)$. $H(x, t)$ is the concentration of the free proton, H^+ .

Solutions $M(x, t)$ and $H_t(x, t)$ of the hyperbolic system, Equations (1) and (2), for variable feeds $\{M(x, t=0), H_t(x, t=0)\}$ remain continuous functions of x and t , or develop into steps. The former solutions are called rarefaction or diffuse waves and the latter shocks or self-sharpening waves (12 - 14). When the steps have developed, the conservation laws become a set of difference equations:

$$\frac{\Delta}{\Delta t} \{ \phi M(x, t) + \underline{M}(M, H) \} + q \frac{\Delta}{\Delta x} M(x, t) = 0, \quad (3)$$

$$\frac{\Delta}{\Delta t} \{ \phi H_t(x, t) + \underline{H}(M, H) \} + q \frac{\Delta}{\Delta x} H_t(x, t) = 0, \quad (4)$$

which in chromatography are called integral coherence conditions as opposed to the differential coherence conditions, Equations (1) and (2) (13).

Temple (19) and Helfferich and Klein (13) have shown that in some circumstances shocks and rarefaction waves coincide when represented in concentration space. This will mainly be the case in this paper.

Riemann Problem and Centered Waves

The solution of the Riemann Problem is the solution of Equations (1) and (2) or Equations (3) and (4) for a single abrupt change (from $\{M_-, H_-\}$ to $\{M_+, H_+\}$) of the chemical composition vector of the feed. Let $x = 0$ be the initial location of this concentration jump, and assume that the pore water flows in positive x -direction:

$$\mathbf{c}(x, t=0) = \begin{cases} \begin{Bmatrix} M_+ \\ H_+ \end{Bmatrix} & \text{for } x \geq 0 \quad (\text{pre-equilibrant}) \\ \begin{Bmatrix} M_- \\ H_- \end{Bmatrix} & \text{for } x < 0 \quad (\text{feed}) \end{cases} \quad (5)$$

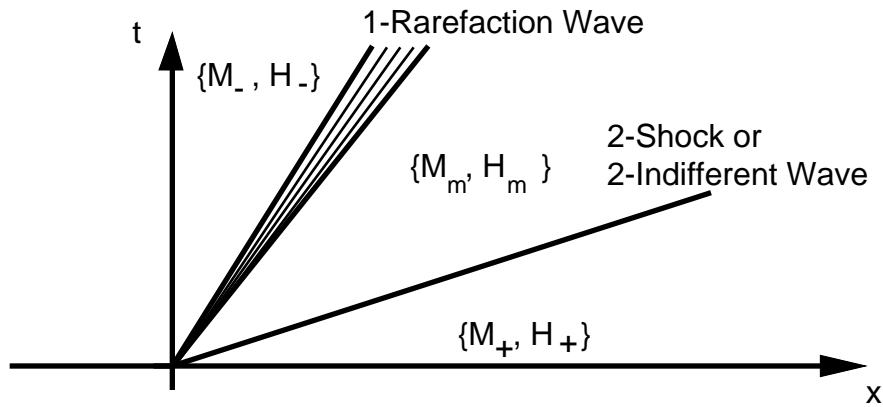


Figure 1: An initial discontinuity between two constant states, $\{M_-, H_-\}$ and $\{M_+, H_+\}$, decomposes with time into a fan of two concentration changes called centered waves, either shocks, indifferent waves or rarefaction waves, separated by the constant state $\{M_m, H_m\}$. Here the 1-wave is plotted as rarefaction wave and the 2-wave as indifferent wave or shock. The notation has been chosen according to conventions in mathematics.

The solution of the Riemann problem Equation (5) is a sequence of constant states separated by centered waves (20) (Figure 1). The constant states are regions of fixed concentrations. The transitions between the constant states are called waves, because each of them is the propagated initial concentration jump, Equation (5). Thus, the term wave is used without implying a periodic variation with time or space.

The heavy lines in Figure 1 are the boundaries of the constant states. The concentration varies from $\{M_-, H_-\}$ to $\{M_m, H_m\}$ across the 1-wave and

from $\{M_m, H_m\}$ to $\{M_+, H_+\}$ across the 2-wave, either continuously as shown for the 1-wave (a rarefaction wave), or abruptly as shown for the 2-wave (an indifferent wave or a shock).

Because all waves originate from the initial discontinuity at $x = 0$, Equation (5), for times $t > 0$ the vector of concentrations $\mathbf{c} = \{M, H_t\}$ in the fan does not depend on x and t separately, but instead on the ratio $\xi = x/t$, the speed of the concentration: a concentration $\mathbf{c}(x,t) = \{M(x, t), H_t(x, t)\}$ is constant on the line $x/t = \xi$, the "characteristic" (light or heavy lines in Figure 1).

The continuous variation of the concentration vector between the concentrations of the two adjacent constant states (heavy lines in Figure 1) is illustrated by drawing a fan of light lines, each representing the path of a concentration \mathbf{c} in (x,t) space (Figure 1). Rarefaction waves expand with time because each concentration propagates with its own speed -hence their name. In an indifferent wave and a shock all concentrations have the same speed. Across these waves the concentration jumps from the constant state on one side to the constant state on the other. This jump is represented by a single heavy line in Figure 1.

These three types of waves will be described in more detail later in this paper.

It is helpful to represent the situation depicted in Figure 1 in concentration space (called "composition space" by Helfferich and Klein (13)), as shown in Figure 2. Constant state $\{M_-, H_-\}$ is connected by the 1-wave to the

middle state $\{M_m, H_m\}$, which in turn is connected by the 2-wave to constant state $\{M_+, H_+\}$.

It will be shown in the section introducing the Jacobian of the isotherms that the 1-rarefaction wave is the curve through the boundary condition $\{M_-, H_-\}$ on which point $\{M_m, H_m\}$ moves when the initial condition $\{M_+, H_+\}$ is varied. Similarly, the 2-rarefaction wave is the curve through the initial condition $\{M_+, H_+\}$ on which point $\{M_m, H_m\}$ moves when the boundary condition $\{M_-, H_-\}$ is varied.

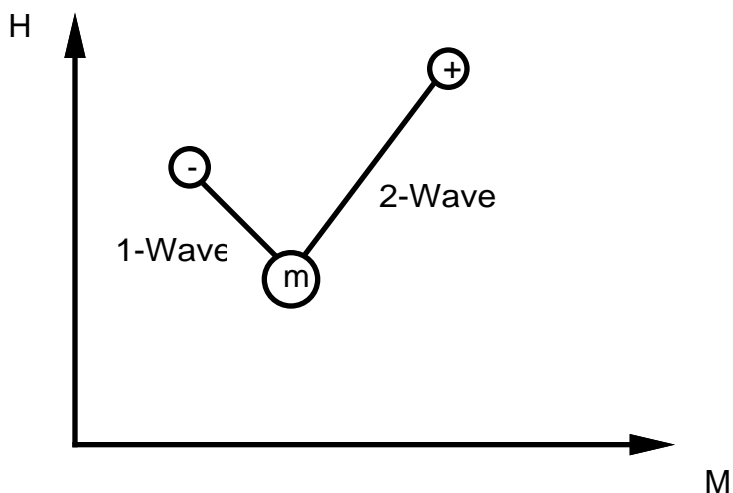


Figure 2: Waves (shown arbitrarily as lines) and constant states (points (-), (m) and (+)) in concentration space. Point (-) has the coordinates $\{M_-, H_-\}$, (+) has the coordinates $\{M_+, H_+\}$, and (m) represents $\{M_m, H_m\}$.

In Figure 2 the waves have been arbitrarily represented as lines. It is the goal of this paper to show how their form depends on the chemical interactions at the adsorbing oxide surface. The first step in that direction is a simplification of the transport equations (1) and (2) based on the fan like structure in Figure 1.

With $\xi = x/t$ and, consequently ,

$$\begin{aligned}\frac{\partial}{\partial x} &= \frac{\partial \xi}{\partial x} \frac{d}{d\xi} = \frac{1}{t} \frac{d}{d\xi} \\ \frac{\partial}{\partial t} &= \frac{\partial \xi}{\partial t} \frac{d}{d\xi} = -\frac{x}{t^2} \frac{d}{d\xi} = -\frac{\xi}{t} \frac{d}{d\xi}\end{aligned}\quad (6)$$

the transport equations (1) and (2) become a set of ordinary differential equations:

$$\left(\frac{q}{\phi} - \xi\right) \frac{d}{d\xi} \underline{M} - \frac{\xi}{\phi} \frac{d}{d\xi} \underline{M} = 0, \quad (7)$$

$$\left(\frac{q}{\phi} - \xi\right) \frac{d}{d\xi} \underline{H}_t - \frac{\xi}{\phi} \frac{d}{d\xi} \underline{H} = 0. \quad (8)$$

where the derivative with respect to ξ expresses the change across the waves, i.e. -in Figure 1- from one characteristic to the other or -in Figure 2- along the lines representing the waves.

In order to solve Equations (7) and (8), we will express the dependent variables H_t , \underline{M} and \underline{H} as functions of the concentrations M and H of the free ions M^{2+} and H^+ . Whereas the function $H_t(H)$ is well known and can be given without comment in the next paragraph, the adsorbed concentrations \underline{M} and \underline{H} follow from mass action laws describing the adsorption process as complex formation between the adsorbent and surface functional groups. They will be explained in the next section.

It is customary in speciation calculations to approximate $H_t(H)$ in pristine water by the difference between the proton and the hydroxyl concentrations, assuming that the concentration of the H_2O complex remains constant with variable pH ($pH = -\log H$):

$$H_t = H - OH = H - \frac{K_w}{H}, \quad (9)$$

where $K_w = 10^{-14}$ (mol/L)².

Surface Complexation on Hydrated Ferric Oxides

Using their Generalized Two-Layer Model of surface complexation, Dzombak and Morel (21) re-fitted two-component adsorption experiments performed with 12 metal cations and 8 metal oxianions with hydrated ferric oxides, Fe_2O_3 (am), as adsorbent. In the experiments, the metal competes only with the proton for surface sites, no third adsorbing component being present.

The Generalized Two-Layer Model is a simplified version of the Triple Layer Model (22, 23). Adsorption is represented as the formation of chemical complexes with high and low affinity sites, X^sO and X^wO , respectively, where X^s and X^w represent the oxide lattice and O is the oxygen layer at the interface between lattice and aqueous solution. The surface sites $X^\alpha O$ carry one negative electronic charge, regardless of their affinity. All surface complexes are located directly on the oxide surface. The

chemical force can bind ions on the surface even if the surface builds up a repulsive electric charge.

The other layer is a diffuse layer of charges, containing all ions present in the aqueous solution. Ions are pulled into this layer by purely electrostatic forces, until their charges neutralize the surface charge accumulated via surface complexation. The concentration of ions of charge z (positive or negative) in the diffuse layer follows a Boltzmann distribution $P(x)$, where x is the distance from the charged surface

$$P(x) = \exp\left(-\frac{zF\psi(x)}{RT}\right) \quad (10)$$

where $\psi(x)$ is the electrostatic potential at distance x from the surface, F is the Faraday constant, R is the molar gas constant, T is the absolute temperature.

The site $X^\alpha O$ can chemically bind (see Figure 3)

- (1) either two protons, forming the complex $X^\alpha OH_2$ which carries one positive charge, or
- (2) one proton, forming the electrically neutral complex $X^\alpha OH$, or
- (3) the doubly positively charged metal ion, forming the complex $X^\alpha OM$ which carries one positive charge.

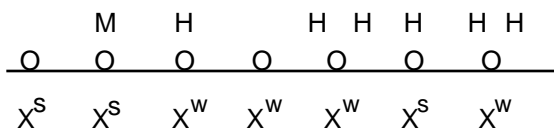


Figure 3: Schematic of surface of oxide lattice (X^s , X^w) with interfacial oxygen layer (O) and some surface complexes (X^sOM , X^sOH , X^wOH , X^wOH_2).

Thus, the total concentration X_T^α of surface sites of type α is the sum of the concentrations of these three surface complexes and $X^\alpha O$:

$$X_T^\alpha = X^\alpha OH_2 + X^\alpha OH + X^\alpha O + X^\alpha OM, \quad (\alpha = s, w), \quad (11)$$

Henceforth, when the symbol X is used without superscript α , the sum of the corresponding expressions is implied, i.e.

$$\begin{aligned} XOH_2 &= X^sOH_2 + X^wOH_2, \\ XOH &= X^sOH + X^wOH, \\ XO &= X^sO + X^wO, \\ XOM &= X^sOM + X^wOM, \\ X_T &= X_T^s + X_T^w. \end{aligned} \quad (12)$$

The surface complex concentrations $X^\alpha L$ in Equations (11) or (12) are the following functions of the free metal ion and proton concentrations, M and H :

$$X^\alpha OH_2(M, H) = X_T^\alpha \frac{k_1 P_0 H^2}{\delta_\alpha} \quad (13)$$

$$X^\alpha OH(M, H) = X_T^\alpha \frac{H}{\delta_\alpha} \quad (14)$$

$$X^\alpha O(M, H) = X_T^\alpha \frac{k_2/P_0}{\delta_\alpha} \quad (15)$$

$$X^{\alpha}OM(M, H) = X_T^{\alpha} \frac{\alpha_{\alpha} P_0 M}{\delta_{\alpha}} \quad (16)$$

where

$$\delta_{\alpha} = \alpha_{\alpha} P_0 M + H (1 + k_1 P_0 H) + \frac{k_2}{P_0}. \quad (17)$$

The proof -given in Appendix I- uses the following two relationships:

(1) the site balance equations (11),

(2) the mass action laws for surface complex formation with the concentrations of the proton and metal ion corrected for electrostatic effects by inclusion of Equation (10), the Boltzmann distribution evaluated at the surface, $P(x=0) = P_0$.

The Boltzmann distribution factor P_0 can be expressed as a function of both the concentration c of the electrolyte, i.e. of the ions in solution, and the concentrations of the surface complexes responsible for surface charge

$$P_0(XOH_2, XO, XOM, c) = \exp\left(-\frac{F\psi_0(XOH_2, XO, XOM, c)}{RT}\right) \quad (18)$$

With Equation (18) Equations (13) - (17) become a set of implicit equations in M and H of the type $X^{\alpha}OL(M, H) = f(M, H, X^{\beta}OK)$, where $X^{\beta}OK$ stands for all surface species. The program DSURF (21), the implementation of the Generalized Two Layer Model, solves these implicit equations numerically for

the surface complex concentrations (13) - (17) as functions of M and H or H_t .

Analytical Solutions Below the Ionic Strength Threshold

The transport equations (7) and (8) are usually solved with a numerical finite difference scheme incorporating the two numerical functions

$$\underline{M}(M, H) = XOM \quad (19)$$

$$\underline{H}(M, H) = XOH + 2 XOH_2 \quad (20)$$

The chromatographic model presented here avoids introducing numerical functions at this point. Instead, the Boltzmann correction factor P_0 is approximated with an analytical function P . At trace concentrations of the metal, P is a function only of pH and the ionic strength I (21),

$$I = \frac{1}{2} \sum_{\substack{\text{all ions } i \\ \text{in solution}}} z_i^2 c_i \quad (21)$$

At small ionic strengths $I \leq 10^{-4}$ mol/L and $\underline{M} \ll X_T$ (pristine water approximation), the correction factor can well be approximated by

$$P = \frac{\sqrt{\frac{k_2}{k_1}}}{H} = \frac{PZC}{H} \quad \text{for } I \leq 10^{-4} \text{ mol/L, } \underline{M} \ll X_T \text{ (pristine water approximation)} \quad (22)$$

as can be seen in Figure 4. At $I = 10^{-1}$ mol/L the approximation

$$P = \left(\frac{PZC}{H}\right)^{2/3} \quad \text{for } I = 10^{-1} \text{ mol/L, } \underline{M} \ll X_T \quad (23)$$

is good for $4 \leq \text{pH} \leq 11$.

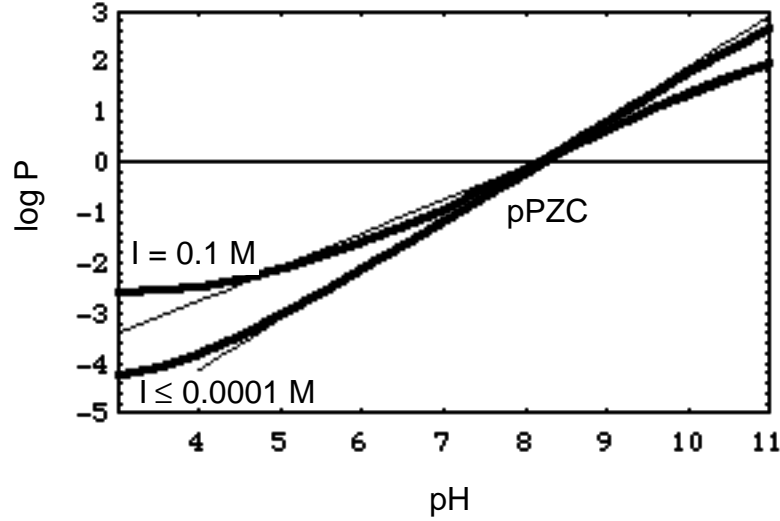


Figure 4: Boltzmann distributions at oxide surface P_0 (heavy lines, Equation (18)) and their analytic approximations $P(\text{pH})$ (light lines, Equations (22) and (23)) as functions of pH at ionic strengths $I = 10^{-4} \text{ mol/L}$ and $I = 10^{-1} \text{ mol/L}$ (from (21)). At $\text{pH} = -\log \text{PZC}$ both P and P_0 are 1.

A property of the pristine water approximation Equation (22) is that the ratios between the surface complex concentrations are constant

$$\frac{X^{\alpha}\text{OH}_2}{X^{\alpha}\text{O}} = 1, \quad \frac{X^{\alpha}\text{OH}_2}{X^{\alpha}\text{OH}} = \sqrt{k_1 k_2} \quad \text{for } I \leq 10^{-4} \text{ M, } X_{\text{OM}} \ll X_T \quad (24)$$

The balance between positive and negative surface charges, $X^{\alpha}\text{OH}_2$ and $X^{\alpha}\text{O}$, at $X_{\text{OM}} \ll X_T$ is equivalent to $\sigma = F(X^{\alpha}\text{OH}_2 - X^{\alpha}\text{O} + 2 X_{\text{OM}}) \approx 0$. This is a property of the electric condenser formed by the surface on one side and

the electrolyte in the diffuse layer on the other and is expressed in Equation (I.11): The reaction enthalpy of surface complex formation is larger or equal to the work necessary to move ions against the repulsive electric potential, i.e. chemistry can only build up a certain surface potential ψ_0 . At fixed ψ_0 in Equation (I.11), σ tends to zero when c approaches zero, i.e. the surface can only hold very little net charge σ .

With Equation (22) we find an analytical solution of the set of transport equations (7) and (8) (proof can be found in Appendix II):

$$M = M_- - (H - H_-) - K_w \left(\frac{1}{H} - \frac{1}{H_-} \right) \quad (\text{1-wave, retarded}), \quad (25)$$

$$H = H_+ \sqrt{\frac{M}{M_+}} \quad (\text{2-wave, non-retarded}). \quad (26)$$

$\{M_-, H_-\}$ is a fixed point, e.g. point (-) in Figure 5, lying anywhere on the solid line $M(M_-, H_-, H)$, the 1-wave Equation (25). Similarly, $\{M_+, H_+\}$ is a fixed point, like (+) in Figure 5, lying anywhere on the dashed line $H(M_+, H_+, M)$, the 2-wave Equation (26).

Thus, in the pristine water approximation, the waves do not depend on any of the adsorption parameters and are therefore element independent. The shape and the slope of the 2-waves are given alone by the requirement of electroneutrality, Equation (24), and the charge of the metal ion. The latter determines the exponent of P_0 in Equation (16) and leads ultimately to the square root in Equation (26). The shape of the 1-waves is given by electroneutrality, Equation (24), and the presence of the soluble OH complex, Equation (9).

At high pH the 1-waves approach the asymptotic line

$$M(M, H, H) = \frac{K_w}{H} \quad \text{for } H \rightarrow 0, M+H_t \ll M+H_t \quad (27)$$

Figure 5 shows the grid of 1- and 2-waves. Helfferich has called this mesh of waves the "street map of the system".

It is stated here without proof that at this low ionic strength, i.e. when Equation (22) is valid, shocks (solutions of Equations (3) and (4)) and rarefaction waves (solutions of Equations (1) and (2)) coincide. Thus, the lines in Figure 5 are both shocks and rarefaction waves.

The retardations $\rho_1(M, H)$ and $\rho_2(M, H)$ of the 1- and 2-rarefaction waves

$$\rho_k(M, H) = \frac{q/\phi}{\xi_k} \quad (28)$$

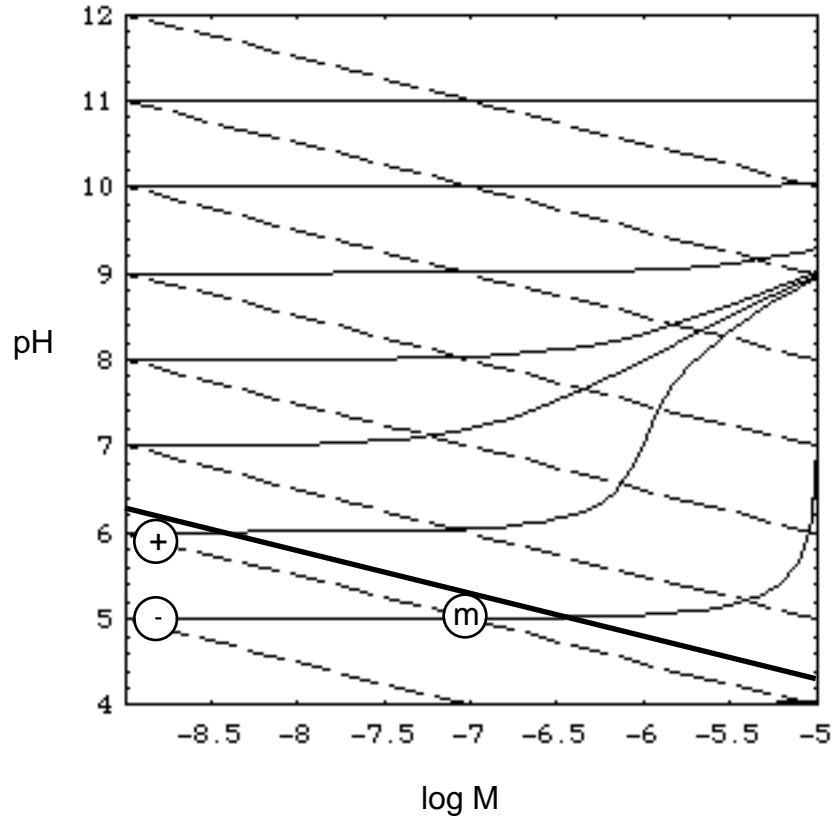


Figure 5: 1- and 2-waves, Equations (25) and (26), in concentration space, calculated with the pristine water approximation Equation (22). 2-waves are dashed. The waves are both rarefaction waves and shocks. Units of M: mol/L. The heavy line is simultaneously a 2-wave and the equivalence line Equation (37). The points (-), (m) and (+) mark the solution of a particular Riemann problem.

can be calculated by solving Equation (7) for $q/(\xi\phi)$ and using the equations for the waves, Equations (25) and (26), to evaluate the expressions (for details of the derivation see Appendix III). The result is

$$\rho_1(M, H) = 1 + \frac{1}{\phi} \frac{\partial XOM(M, H)}{\partial M} \left(1 + \frac{2HM}{H^2 + K_w} \right), \quad (29)$$

$$\rho_2(M, H) = 1$$

where

$$\frac{\partial XOM(M, H)}{\partial M} = X_T \frac{\alpha \text{PZC} (1 + 2 k_1 \text{PZC}) H^2}{(\alpha \text{PZC} M + H^2 (1 + 2 k_1 \text{PZC}))^2}. \quad (30)$$

Within the 1-rarefaction wave each concentration $\{M, H\}$ propagates with its own speed $\xi_1 = q/(\phi \rho_1(M, H))$. The fan of characteristics expands with time (see Figure 1). All concentrations in the 2-wave propagate with the same unretarded speed $\xi_2 = q/\phi$ (see Equations (28) and (29)). It is an indifferent wave.

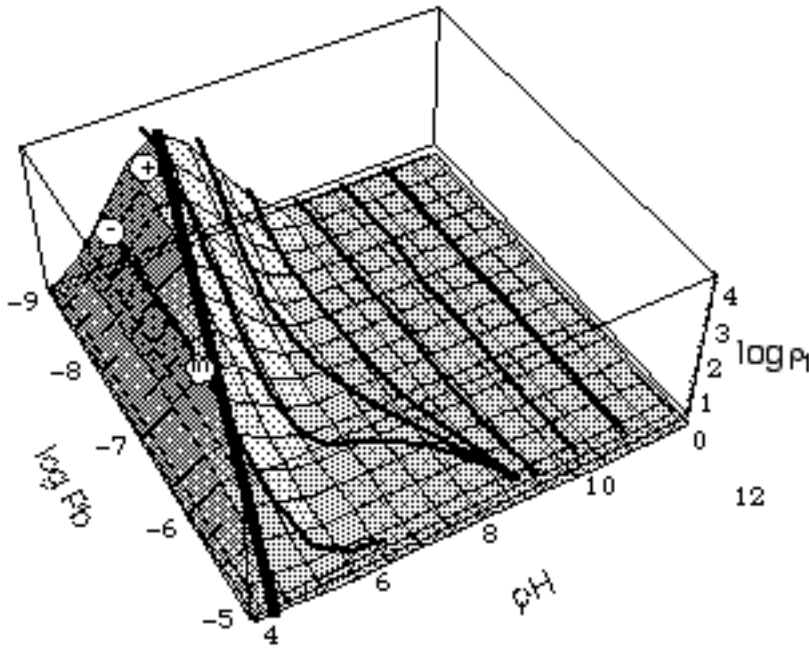


Figure 6: 1-waves, Equation (25), superimposed on corresponding retardation surface $\rho_1(\text{Pb}, H)$, Equations (29) and (30), for Pb/H system at ionic strength $I \leq 10^{-4}$ mol/L. Units of Pb: mol/L. The heavy line is simultaneously the equivalence line, Equation (37), and a 2-wave, Equation (26). The points (-), (m) and (+) mark the solution of a particular Riemann problem. (Here are the corresponding 1-waves in V.

Prigiobbe's paper (27):

http://acamedia.info/sciences/J_G/sichtF/prigiobbe13_slow_wave.jpg:

Figure 6 shows the 1-rarefaction waves of Figure 5 superimposed on the surface $\rho_1(M, H)$. Whereas the waves are element independent, the retardations are not. The retardation surface was calculated for the Pb/H system with hydrous ferric oxide as adsorbent ($\alpha_s = 10^{-4.65}$, $\alpha_w = 0$, PZC = $10^{-8.1}$ mol/L, $k_1 = 10^{7.3}$ L/mol, after (21)).

Waves Above the Ionic Strength Threshold: The Jacobian of the Isotherms

At higher ionic strengths, e.g. $I = 0.1$ M, the solution method for the set of transport equations (7) and (8) is based on the Jacobi matrix of the adsorption isotherms $\underline{M}(M, H)$ and $\underline{H}(M, H)$, Equations (19) and (20), as is described in detail in Appendix IV. With $\mathbf{c} = \{M, H_t\}$, the retardations $\rho_1(\mathbf{c})$ and $\rho_2(\mathbf{c})$ of the rarefaction waves are the eigenvalues of the retardation matrix

$$\underline{R}(\mathbf{c}) = \underline{I} + \frac{1}{\phi} \underline{Kd}(\mathbf{c}) \begin{bmatrix} 1 & 0 \\ 0 & \frac{\partial H}{\partial H_t} \end{bmatrix} \quad (31)$$

where the matrices \underline{I} and $\underline{Kd}(\mathbf{c})$, the unit matrix and Jacobian of the isotherms, respectively, are

$$\underline{I} = \begin{bmatrix} 1 & 0 \\ 0 & 1 \end{bmatrix},$$

$$\underline{\mathbf{Kd}}(\mathbf{c}) = \begin{bmatrix} \frac{\partial}{\partial M} \text{XOM}(\mathbf{c}) & \frac{\partial}{\partial H} \text{XOM}(\mathbf{c}) \\ \frac{\partial}{\partial M} (2\text{XOH}_2(\mathbf{c}) + \text{XOH}(\mathbf{c})) & \frac{\partial}{\partial H} (2\text{XOH}_2(\mathbf{c}) + \text{XOH}(\mathbf{c})) \end{bmatrix} \quad (32)$$

The matrix $\{\{1, 0\}, \{0, \partial H/\partial H_t\}\}$ is a consequence of the isotherms being functions of M and H whereas the dependent variables in the transport equations are M and H_t .

At any point $\mathbf{c} = \{M, H_t\}$ the retardation matrix has two retardation eigenvalues $\rho_1(\mathbf{c})$ and $\rho_2(\mathbf{c})$. The system is non-degenerate, i.e.

$$\rho_1(\mathbf{c}) > \rho_2(\mathbf{c}) \geq 1. \quad (33)$$

It is shown in Appendix IV that the 1- and 2-rarefaction waves are the curves that are everywhere tangential to the eigenvectors $\mathbf{r}_1(\mathbf{c})$ and $\mathbf{r}_2(\mathbf{c})$ of the Jacobian $\underline{\mathbf{Kd}}(\mathbf{c})$, respectively. They can be constructed from the corresponding eigenvector field $\mathbf{r}_k(\mathbf{c})$ by a suitable integration method, such as the Euler or a Runge-Kutta method (see Appendix IV). The latter is incorporated in the high level computer language AVS (Application Visualization System (24)). After having received the vector field $\mathbf{r}_k(\mathbf{c})$ from the user, AVS constructs the k-wave on the computer screen, when the user presses the corresponding button.

Convention Equation (33) is built upon an important property of the system, its genuine non-linearity.

Genuine Non-Linearity and The Equivalence Line

The system is genuinely nonlinear in those regions of concentration space where the retardation varies across the waves. Let $\rho_k(\mathbf{c})$ be the retardation of the k-wave, then at every point \mathbf{c} in concentrations space such a system has obviously the property

$$(\text{grad } \rho_k, \mathbf{r}_k) = \left\langle \left\{ \frac{\partial \rho_k}{\partial M} \quad \frac{\partial \rho_k}{\partial H_t} \right\}, \mathbf{r}_k \right\rangle \neq 0 \quad (34)$$

The retardation has a local maximum when half the number of sites are occupied by metal ions, i.e. when in the isotherms (19), (20) with Equations (13) - (17) the term $\alpha_\alpha P_0 M$ equals one half the size of the denominator δ_α .

$$\alpha_\alpha P_0 M = H (1 + k_1 P_0 H) + \frac{k_2}{P_0} \quad (35)$$

Solving for M gives the equation of what we will call "equivalence line for site type α ":

$$M_{\text{eq}}^\alpha = \frac{\frac{k_2}{P_0} + H (1 + k_1 P_0 H)}{\alpha_\alpha P_0} \quad (36)$$

Replacing P_0 with the pristine water approximation (22) gives the heavy lines in Figures 5 and 6

$$M_{\text{eq}}^\alpha = \frac{1}{\alpha_\alpha \text{PZC}} H^2 (1 + 2k_1 \text{PZC}) \quad (37)$$

Waves at Elevated Ionic Strength: The Equivalence Threshold

The Pb/H system is used here to demonstrate how the grid of waves is deformed relative to the element independent pattern in Figures 5 and 6, when a higher ionic strength allows the oxide surface to pick up electronic charge in the adsorption process. The adsorption parameters used for the calculation of the Jacobi or retardation matrix are (21):

Adsorption and desorption of a proton:

$$\begin{aligned} k_1 &= 10^{7.3} \text{ L/mol} \\ k_2 &= 10^{-8.9} \text{ mol/L} \end{aligned} \quad (38)$$

Adsorption of lead:

$$\begin{aligned} \alpha_s &= 10^{4.65} \\ \alpha_w &= 0 \text{ (only high affinity sites bind Pb)} \end{aligned} \quad (39)$$

Figure 7 displays the 1- and 2-rarefaction waves. Comparing this with Figure 5, we see that below the equivalence line Equation (36), the heavy line in Figure 7, the waves are similar to the ones in Figure 5. This indicates an exchange behavior similar to the one in Figure 5: lead and proton compete for adsorption sites similarly as in the low ionic strength approximation. This is the reason why here shocks and rarefaction waves nearly coincide, which they precisely do in Figure 5.

Above the equivalence line, the system in Figure 7 has decoupled: The 1-wave is the proton wave, the 2-wave is the lead wave. In the decoupled system shocks and rarefaction waves run parallel to the axes, which means

that Equations (7) and (8) decouple: In a wave, whether shock or rarefaction wave, only one component varies..

So, shocks and rarefaction waves coincide everywhere in concentration space, except in the transition region near the equivalence line.

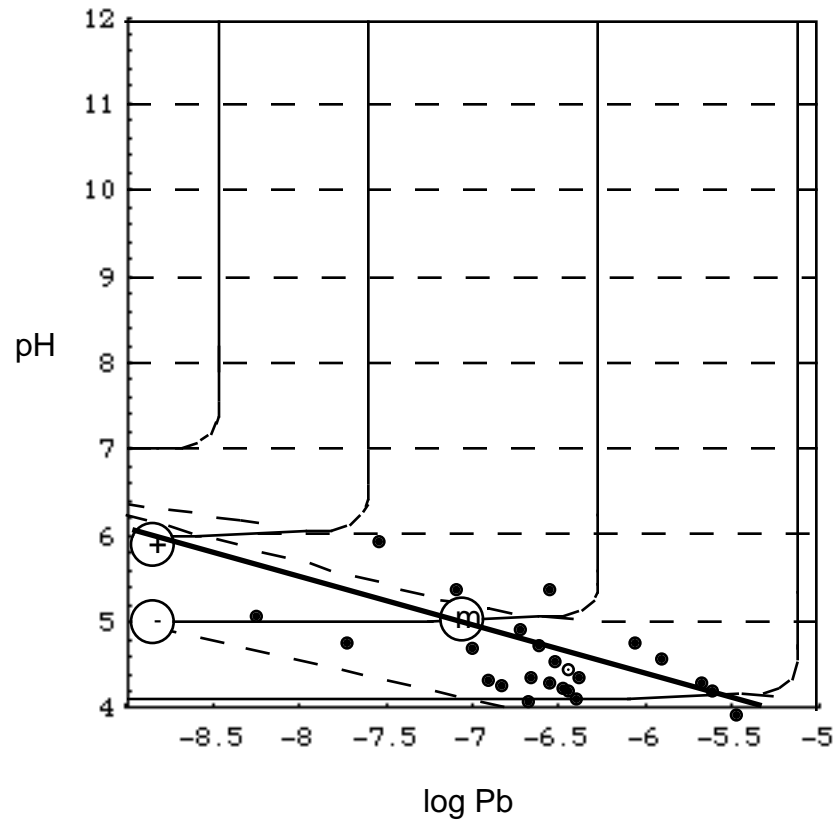


Figure 7: 1- and 2-waves for the system Pb/H at ionic strength $I = 0.1$ mol/L. 2-waves are dashed. Units of Pb: mol/L. The heavy line is simultaneously a 2-wave and the equivalence line Equation (36). The points (-), (m) and (+) mark the solution of a particular Riemann problem. The adsorption constants are based on experiments performed in a system with $I = 0.1$ mol/L at the positions marked by dots.

The decoupling at high pH is interpreted as follows: The Pb ions occupy all high affinity sites as they win in competition with the protons, which bind

much more weakly to these sites. Thus, only the low affinity sites are left to the protons. To those sites Pb ions have no access ($\alpha_w = 0$). Thus, protons and Pb ions do not compete or exchange with each other when they adsorb in the region above the equivalence line, except for the electrostatic interactions which are weak because of the non vanishing ionic strength.

Adsorption experiments from which Dzombak and Morel (21) extracted the adsorption data (38) and (39) have been performed at $I = 0.1$ mol/L and at the positions marked by the dots in Figure 7. Because of the nonlinearity of the adsorption model Equations (13) - (17), adsorption data are valid only within the thresholds in concentration space where they were determined i.e. in the region where protons exchange with Pb ions upon adsorption. The validity of the chosen adsorption data was neither checked in the region where the system decouples nor for the pristine water system ($I \leq 10^{-4}$ mol/L, $M \ll X_T$).

Figure 8 shows the waves superimposed on the retardation $\rho_i(M, H)$. By definition, a wave is a rarefaction wave, when its front part propagates faster than its rear end, resulting in a profile $c(x, t)$ that spreads with time. When the rear end of a wave is faster than its front it runs into the front and a shock forms. Therefore, Figure 8 helps us decide when a wave is a rarefaction wave: we have a rarefaction wave only when the front end of the wave is downhill from its rear end. Thus, the 1-wave in the Riemann problem in Figure 7 is a rarefaction wave, and the 2-wave is a shock.

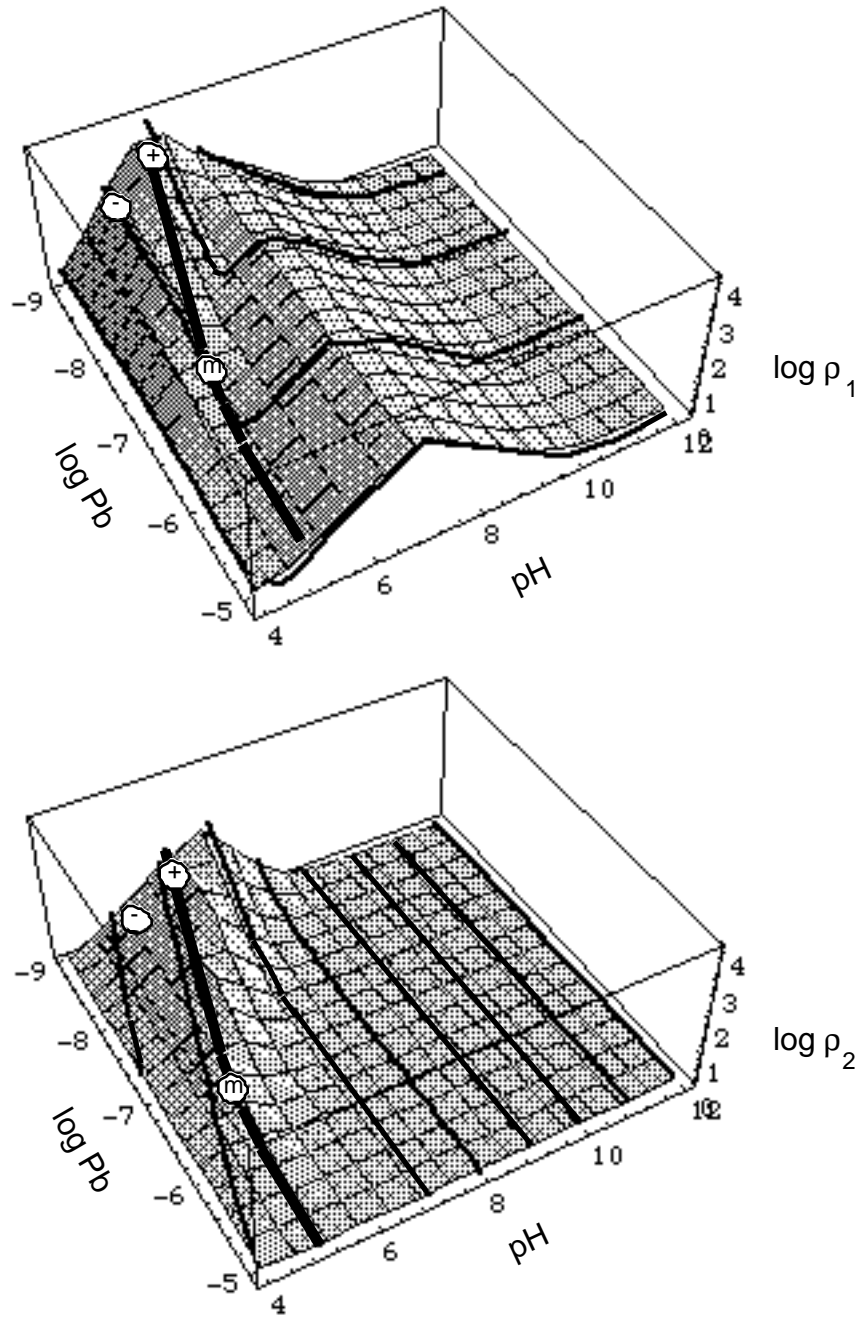


Figure 8: 1-waves (upper picture) and 2-waves (lower picture), Equations (IV.17) - (IV.19), for system Pb/H at ionic strength $I = 0.1$ M, superimposed on the corresponding retardation surface $\rho_1(\text{Pb}, \text{H})$ and $\rho_2(\text{Pb}, \text{H})$, respectively, defined in Equations (31) - (32). Units of Pb: mol/L. The heavy line is simultaneously the equivalence line Equation (36) and a 2-wave. The points (-), (m) and (+) mark the solution of a particular Riemann problem.

The shocks are calculated from Equations (3) and (4) as demonstrated in detail in Appendix V. Figure 9 shows some 2-shocks of the Pb/H system at ionic strengths $I = 0.1$ mol/L. As pointed out above, they deviate from the 2-rarefaction waves (Figure 7) near the equivalence line, but this deviation does not change the geometrical structure of the remobilization scenario represented by the Riemann problem in Figures 5 - 8. Therefore, in the following section the metal accumulation during a remobilization scenario will be discussed for the pristine water approximation of the waves.

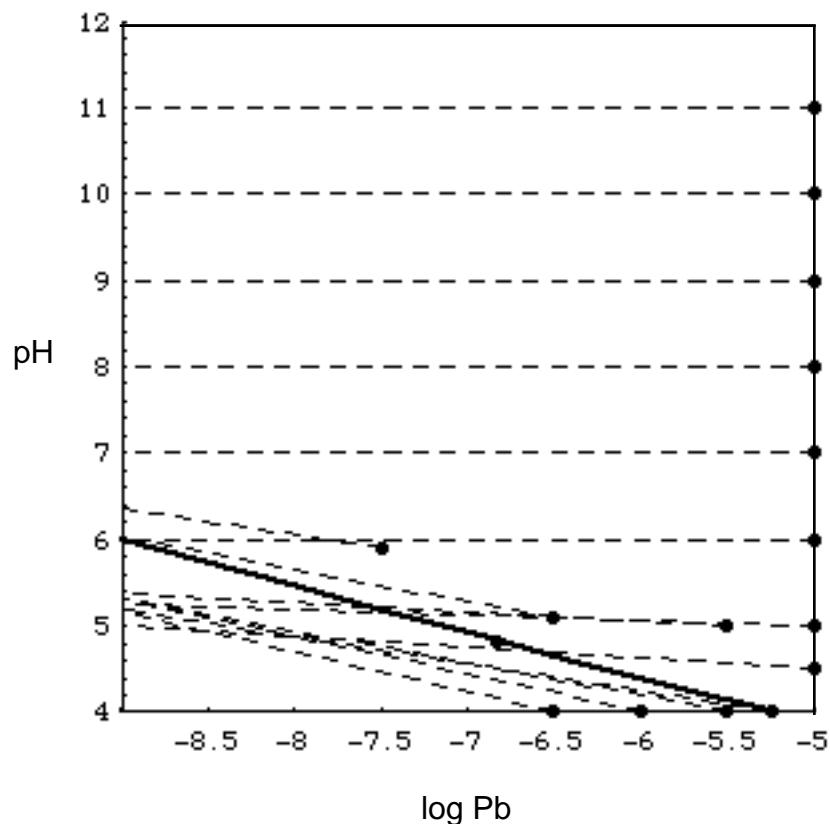


Figure 9: 2-shocks, solutions of Equations (3) and (4), for the system Pb/H at ionic strength $I = 0.1$ mol/L. Units of Pb: mol/L. Point (m) of the shock is marked by a dot. The heavy line is simultaneously the equivalence line Equation (36) and a 2-shock.

Metal Accumulation Between Waves

The distance $x_k(\mathbf{c})$, a concentration $\mathbf{c} = \{M, H\}$ in the k-wave has traveled at time t , is by definition of the retardation ρ_k in Equation (28)

$$x_k(\mathbf{c}) = \xi_k(\mathbf{c}) t = \frac{q t}{\phi \rho_k(\mathbf{c})}, \quad (40)$$

where $\xi_k(\mathbf{c})$ is the speed of the concentration \mathbf{c} in the k-wave. The pristine water approximation of the concentration profile x_1 of the 1-wave results when in $\mathbf{c} = \{M, H\}$ the variable M is replaced with the function M given in Equation (25)

$$x_1(\{M(M, H, H), H\}) = \frac{q t}{\phi \rho_1(\{M(M, H, H), H\})} \quad \text{for } H = H. \dots H_m \quad (41)$$

and Equation (29) with Equation (30) are used to define the retardation ρ_1 . In the 2-wave all concentrations have the same retardation $\rho_2(\mathbf{c}) = 1$ (see Equation (29)). It is an indifferent wave. Thus, within the 2-wave $H(M_+, H_+, M)$, Equation (26), the concentration vector jumps at $x = x_2$ from $\{M_m, H_m\}$ to $\{M_+, H_+\}$. The concentration profile is

$$x_2(\{M, H(M_+, H_+, M)\}) = \frac{q t}{\phi} \quad \text{for } M = M_m \dots M_+ \quad (42)$$

Figure 10 shows the 1- and 2-waves in the pristine water approximation, Equation (22), for three Riemann problems representing remobilization of an initially poorly soluble lead inventory, $\{M_+, H_+\} = \{10^{-8.8}, 10^{-6} \dots 10^{-8}\}$ mol/L.

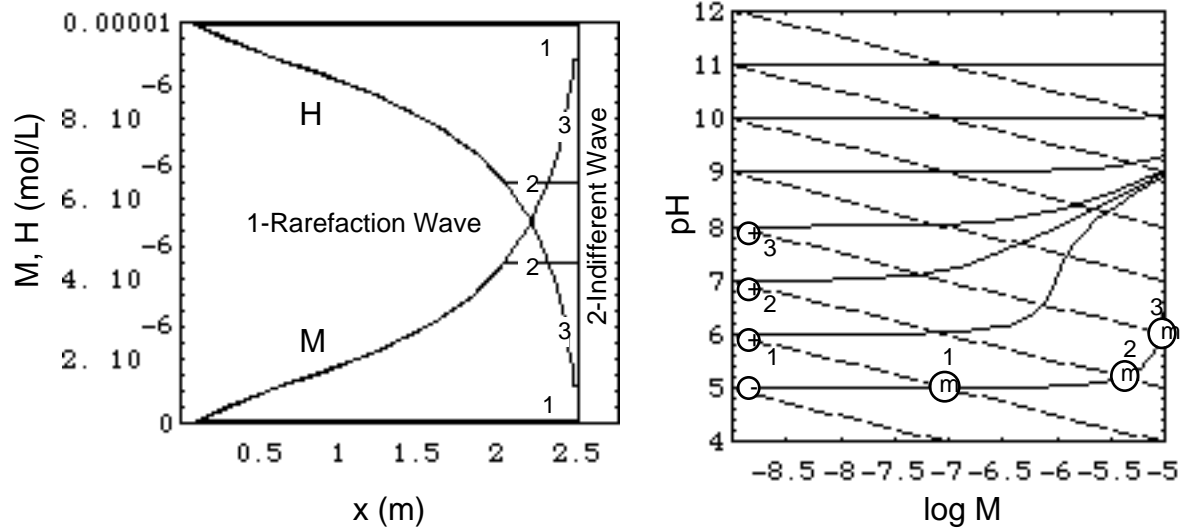


Figure 10: Waves (1-rarefaction wave, Equation (25), and 2-indifferent wave, Equation (26), right) and concentration profiles (left), Equations (41) and (42), for three Riemann problems calculated for $I \leq 10^{-4}$ M, $\phi = 0.4$, $q t = 1$ m. Adsorption data (21) given in Equations (38) and (39). Feed water composition is the same for all three Riemann problems, i.e. point (-) in plot of waves on the right. In plot of profile, constant state (m) is clearly visible only in Riemann problem 2, whereas in problem 3 it has vanishing width (from $x = 2.47$ m to 2.5 m), and in problem 1 it extends over almost the entire length of the profile (from $x = 0.1$ m to 2.5 m), its metal and proton concentrations nearly coinciding with the frame of the plot.

In addition to Equations (38) and (39) the following data have been used in the calculations:

$$\phi = 0.4, q t = 1 \text{ m} \quad (43)$$

The waves are plotted both in concentration space (right hand side of Figure 10) and in physical space (on the left). The water flows in positive x-

direction. In Riemann problem 1 the 1-rarefaction wave extends over a very small portion of the profile,

$$x_1(\{M(M, H_-, H_m), H_m\}) = 0.11 \text{ m} \quad (44)$$

in problem 3 it covers almost the entire profile:

$$x_1(\{M(M, H_-, H_m), H_m\}) = 2.47 \text{ m}, \quad (45)$$

Only in problem 2 the intermediate constant state $\{M_m, H_m\}$ is clearly visible

$$x_1(\{M(M, H_-, H_m), H_m\}) = 2.03 \text{ m} \quad (46)$$

The 2-wave is a nonretarded indifferent wave, and its concentration profile is

$$x_2(\{M, H(M_+, H_+, M)\}) = 2.5 \text{ m} \quad \text{for } M = M_m \dots M_+, \quad (47)$$

The constant state $\{M_m, H_m\}$ extends between the boundaries of the 1- and 2-waves, i.e. from $x_1(\{M(M_-, M_-, H_m), H_m\})$ to $x_2(\{M, H(M_+, H_+, M), H\})$.

The proton and lead concentrations in the 1-wave are symmetrical about the line at $M = 0.5 (M_- + H_-)$, because in Equation (25) with $H \gg \sqrt{K_w}$, we have -typical of an exchange process in a two-component system

$$M = (M_- + H_-) - H, \quad (48)$$

The reason why the lead ions accumulate, is this: Behind the 1-wave, the protons have displaced metal ions from the adsorbing surface, because $H_- > H_+$. The remobilized metal ion inventory is compressed between the front of intruding water, $x(M_-, H_-)$, and the 2-wave, because in front of the 2-wave we have -by definition of the 2-wave- the original state of the column characterized by $\mathbf{c}_+ = \{M_+, H_+\}$.

The relocated metal concentration increases when the widths of the 1-wave and the constant state $\{M_m, H_m\}$ decrease. The width of the latter constant state decreases when the speeds $\xi_1(\{M_m, H_m\})$ and $\xi_2(\{M_m, H_m\}) = q/\phi$ of its two bordering characteristics approach each other, or in other words $\rho_1(\{M_m, H_m\})$ approaches 1. In Figure 6 one can see that this is the case when point (m) moves to the right. Therefore accumulation of the metal ion increases from Riemann problem 1 to 3.

Conclusions and Outlook

Concentration profiles of lead and protons have been derived from the chemical interactions. Lead ions and protons bind chemically to the oxide surfaces which present a high and a low affinity adsorption site type. Lead binds probably only to the minority sites, i.e. the high affinity type. Because protons adsorb on both site types, particularly on the majority sites, in a wide region of concentration space there is little competition between lead and protons for adsorption sites, except

- (a) when electrical forces counteracting the chemical surface bond confine the variation of the electric surface charge to a narrow range,

thus forcing upon the system a behavior known from ion exchange systems (ionic strength threshold).

(b) -in the absence of (a)- near a threshold and on the low pH side of it, i.e. a line in concentration space where half the high affinity sites are filled with lead ions (equivalence line threshold).

The calculations in this paper have shown that the waves in a system with competition have the same geometrical shape as in ion exchange systems. Thus, in all cases of competition the accumulation of lead after its remobilization from the oxides surface is similar to a process known as displacement development with which ion exchange resins are regenerated (13).

The adsorption data (21) were derived from experiments performed at $I = 0.1$ mol/L and below or near the equivalence threshold Equation (36). With Helfferich's street map it has been shown that the applicability of the data has to be checked in those cases where the waves are separated by thresholds (a) or (b) from the experimentally probed region.

The behavior of hyperbolic systems, such as the one presented here, has been intensively studied for many decades. We often know which systems have easy and transparent solutions. The waves and retardations derived from the conserved quantities, i.e. the total soluble and the adsorbed concentration, or calculated from the Jacobian matrix of the isotherms are such simple solutions. Such chromatographic solution methods provide an efficient and simple means of orientation in a new transport system, similar

to the well known methods that have been used to interpret the speciation in batch systems (25).

The calculations can be done e.g. in high-level languages such as Mathematica (26) on a Macintosh or a Personal Computer and AVS (Application Visualization System (24)) on a workstation and take typically several minutes computing time. They can thus be integrated in the work of a chemical laboratory and help locate batch experiments in concentration space that aim at the determination of adsorption constants.

Acknowledgment

Part of this research was done while the author was visiting member of the Courant Institute of Mathematical Sciences of New York University, New York. Without the long discussions with F. Helfferich of The Pennsylvania State University this work would not have been possible.

Nomenclature

First parentheses give units. (-) means dimensionless.

Last parentheses give number of equation or Figure where symbol first appears or is defined.

c	electrolyte concentration (mol per Liter of liquid), (18),
c	vector of soluble concentration $\{M, H_t\}$ or $\{M, H\}$, (mol per Liter of liquid), (31),
F	Faraday constant (96485 Coulomb per mol), (10),
H ₊	$H(x \geq 0, t = 0)$, (5),
H ₋	$H(x < 0, t = 0)$, (5),

- H_{t-} $H_t(x < 0, t = 0)$, (27), see also (9),
- H_m concentration of free proton between 1- and 2-wave, (mol per Liter of liquid), (Figure 1),
- $H_t(x, t)$ total soluble concentration of protons, (mol per Liter of liquid), (2),
- $H(\xi)$ concentration of free proton, (mol per Liter of liquid), (8),
- $H(x, t)$ concentration of free proton at location x and time t , (mol per Liter of liquid), (9),
- $\underline{H}(M, H)$ adsorbed proton concentration (proton isotherm), (mol per Liter of system volume), (2),
- I ionic strength, (mol per Liter of liquid), (21),
- \underline{I} identity matrix, (32),
- k index specifying wave, $k = 1$: 1-wave (slow), $k = 2$: 2-wave (fast), (Figure 1, (25), (26)),
- k_1 equilibrium formation constant of XOH_2 surface complex from XOH and H , ($10^{7.3}$ Liter per mol), (13), (38)
- k_2 equilibrium formation constant of XO surface complex from XOH and H , ($10^{-8.9}$ mol per Liter), (15), (38)
- K_w water dissociation constant, (10^{-14} (mol per Liter of liquid)²), (9),
- $\underline{Kd}(\mathbf{c})$ Jacobi matrix of isotherms evaluated at location \mathbf{c} in composition space, (-), (32),
- M_+ $M(x \geq 0, t = 0)$, (mol per Liter of liquid), (5),
- M_- $M(x < 0, t = 0)$, (mol per Liter of liquid), (5),
- $\underline{M}(M, H)$ adsorbed metal concentration (metal isotherm), (mol per Liter of system volume), (1),
- $M(x, t)$ soluble metal concentration, (mol per Liter of liquid), (1),
- $M(\xi)$ soluble concentration of metal, (mol per Liter of liquid), (7),
- M_m concentration of metal between the 1- and 2-wave, (mol per Liter of liquid), (Figure 1),

- $M_{eq}^{\alpha}(H)$ soluble equivalent metal concentration (at which half the adsorption sites of type α are filled with metal ions) as a function of H , (mol per Liter of liquid), (36),
- $P(x)$ Boltzmann distribution as a function of distance from oxide surface, (-), (10),
- $P(H)$ analytical approximation of Boltzmann distribution at oxide surface as a function proton concentration, (-), (22), (23)
- $P_0(XO_{..}, c)$ Boltzmann distribution at oxide surface as a function of non neutral surface complex concentrations and electrolyte concentration, (-), (18),
- PZC point of zero charge on hydrous ferric oxide in pristine water, i.e. at $I \leq 10^{-4}$ mol/L
 $PZC = \sqrt{(k_2/k_1 = 10^{-8.1} \text{ mol/L})}$, (22), page 21,
- q flux of water in column of porous medium, (meter per year), (1),
- R molar gas constant, (8.314 Joule per(mol Kelvin)), (10),
- $\underline{R}(c)$ retardation matrix evaluated at location c in concentration space, (-), (31),
- $r_k(c)$ right eigenvector of $\underline{R}(c)$ corresponding to eigenvalue $\rho_k(c)$, ((mol year) per (Liter meter)), (IV.13),
- t time variable, (year), (1),
- T absolute temperature, (Kelvin), (10),
- X_T^{α} concentration of adsorption sites of type α , (mol per Liter of system volume), (11),
- X_T concentration of adsorption sites of any type, (mol per Liter of system volume), (12),
- $X^{\alpha 0}$ concentration of empty sites of type α , (mol per Liter of system), (11),
- $X^{\alpha OL}$ concentration of sites of type α covered with $L = H, H_2, M$, (mol per Liter of system), (11),
- XOL concentration of any site type covered with $L = H, H_2, M$, (mol per Liter of system), (12),
- x space variable (meter), (1),
- z charge of ion, (multiple of unit electronic charge), (10).

α	site type, ($\alpha = s, w$), (11),
α_α	metal-proton exchange constant for site type α , (-), $\alpha_s = 10^{4.65}$, $\alpha_w = 0$, (39)
δ_α	denominator in adsorption isotherms (17), (mol per Liter of liquid),
Δc	concentration jump across shock, (mol per Liter of liquid), (3)
Δt	time interval, (year), (3),
Δx	distance traveled by shock during period Δt , (meter), (3),
ϕ	porosity of medium, (-), (1),
$\rho(\mathbf{c})$	eigenvalue of $\underline{R}(\mathbf{c})$, also called "retardation", (-), (IV.3),
$\rho_k(\mathbf{c})$	retardation of k-rarefaction wave, (-), (33),
σ_k	retardation of k-shock, (-), (V.2),
ξ	speed of concentration \mathbf{c} , (meter per year), (6),
ξ_k	speed of concentration in a k-wave, (meter per year), (28),
$\psi(x)$	electrostatic potential at distance x from oxide surface, (Volt), (10).

Literature Cited

(1) Kirkner, D.J.; Reeves, H. Multicomponent Mass Transport with Homogeneous and Heterogeneous Chemical Reactions: The Effect of the Chemistry on the Choice of Numerical Algorithm, Part 1: Theory. *Water Resour. Res.* 1988, 24, 1719,

(2) Reeves, H.; Kirkner, D.J. Multicomponent Mass Transport with Homogeneous and Heterogeneous Chemical Reactions: The Effect of the Chemistry on the Choice of Numerical Algorithm, Part 2: Numerical Results. *Water Resour. Res.* 1988, 24, 1730,

- (3) Kinzelbach, W.; Schäfer, W.; Herzer J. Numerical Modeling of Nitrate Transport in a Natural Aquifer. in: *Contaminant Transport in Groundwater*, edited by H. Kobus and W. Kinzelbach, pp. 191-198, Balkema: Rotterdam, 1989.
- (4) Lichtner, P.C. Time-Space Continuum Description of Fluid/Rock Interaction in Permeable Media. *Water Resour. Res.* 1992, 28(12), 3135,
- (5) Ortoleva, P.; Merino, E.; Moore, G.; Chadam, J. Geochemical Self-Organization I: Reaction-Transport Feedbacks and Modeling Approach. *Am. J. Sci.* 1987, 287, 979,
- (6) Walsh, M.P.; Bryant, S.L.; Schechter, R.S.; Lake, L.W. Precipitation and Dissolution of Solids Attending Flow Through Porous Media. *AIChE J.* 1984, 30, 317,
- (7) Cederberg, G.A.; Street, R.L.; Leckie, J.O. A Groundwater Mass Transport and Equilibrium Chemistry Model for Multicomponent Systems. *Water Resour. Res.* 1985, 21, 1095,
- (8) Novak, C.F.; Schechter, R.S.; Lake, L.W. Rule-Based Mineral Sequences in Geochemical Flow Processes. *AIChE Journal* 1988, 34, 1607,
- (9) Berninger, J.A.; Whitley, R.D.; Zhang, X.; Wang, N.-H. L. A Versatile Model for Simulation of Reaction and Nonequilibrium Dynamics in Multicomponent Fixed-Bed Adsorption Processes. *Computers chem. Engng.* 1991, 15, 749,

- (10) Liu, T.-P. Hyperbolic Conservation Laws with Relaxation. *Commun. Math. Phys.* 1987, 108, 153,
- (11) Morel, F.M.M. *Principles of Aquatic Chemistry*; Wiley: New York, 1983,
- (12) Lax, P.D., *Hyperbolic Systems of Conservation Laws and the Mathematical Theory of Shock Waves*; SIAM: Philadelphia, 1973,
- (13) Helfferich, F.; Klein, G. *Multicomponent Chromatography - Theory of Interference*; Marcel Dekker: New York 1970,
- (14) Rhee, H-K.; Aris R.; Amundson, N.R. *First-Order Partial Differential Equations: Volume II, Theory and Application of Hyperbolic Systems of Quasilinear Equations*; Prentice Hall: Englewood Cliffs, 1989,
- (15) Schweich, D.; Sardin, N.R.; Jauzein, M. Properties of Concentration Waves in Presence of Nonlinear Sorption, Precipitation/Dissolution, and Homogeneous Reactions, 1. Fundamentals, 2. Illustrative Examples. *Water Resour. Res.* 1993, 29, 723,
- (16) Helfferich, F., Multicomponent Ion-Exchange in Fixed Beds. *Ind. Eng. Chem. Fundam.* 1967, 6, 362,
- (17) Hwang, Y.-L.; Helfferich, F.G.; Leu, R.-J. Multicomponent Equilibrium Theory for Ion-Exchange Columns Involving Reactions, *AIChE J.* 1988, 34, 1615,

- (18) LeVeque, R. J., *Numerical Methods for Conservation Laws*; Lectures in Mathematics, ETH Zürich, Birkhäuser: Basel, 1991,
- (19) Temple, B. Systems of Conservation Laws with Invariant Submanifolds. *Trans. Amer. Math. Soc.* 1983, 2, 781,
- (20) Lax, P.D. Hyperbolic Systems of Conservation Laws II, *Comm. Pure Appl. Math.* 1957, 10, 537,
- (21) Dzombak, D.A.; Morel, F.M.M. *Surface Complexation Modeling: Hydrous Ferric Oxide*; Wiley: New York, 1990,
- (22) Davis, J.A.; James, R.O.; Leckie, J.O. Surface Ionization and Complexation at The Oxide/Water Interface: 1. Computation of Electric Double Layer Properties in Simple Electrolytes. *J. Colloid Interface Sci.* 1978, 63, 480,
- (23) Davis, J.A.; Leckie, J.O. Surface Ionization and Complexation at The Oxide/Water Interface: 2. Surface Properties of Amorphous Iron Oxyhydroxide and Adsorption of Metal Ions, *J. Colloid Interface Sci.* 1978, 67, 90,
- (24) International AVS Center, North Carolina Supercomputing Center, P.O. Box 12889, 3021 Cornwallis Road, Research Triangle Park, North Carolina, NC 27709, telnet: avs.ncsc.org.
- (25) Stumm, W.; Morgan, J.J. *Aquatic Chemistry*, 2nd ed., Wiley: New York 1981,

(26) Wolfram Research, Inc., *Mathematica, Version 2.2*, Wolfram Research, Inc., 100 Trade Center Drive, Champaign, Illinois, IL 61820-7237, U.S.A. E-Mail: info@wri.com, 1992.

(27) Prigiobbe, V.; Hesse, M., and Bryant, S.L. Hyperbolic Theory for Flow in Permeable Media with pH-dependent Adsorption, *J. Appl. Math.* 73, 5, 1941-1957, Society for Industrial and Applied Mathematics, 2013, E-Mail: valentina.prigiobbe@austin.utexas.edu

Appendices

Appendix I: Charge Dependent Surface Complex Concentrations

The mass action laws for the formation of the surface complexes are

$$X^{\alpha}OH_2 = k_1 X^{\alpha}OH H_0 \quad (I.1)$$

$$X^{\alpha}O = k_2 X^{\alpha}OH \frac{1}{H_0} \quad (I.2)$$

$$X^{\alpha}OM = \alpha_{\alpha} X^{\alpha}OH \frac{M_0}{H_0}, \quad (I.3)$$

where k_1 , k_2 , the ad- and desorption constants for a proton, are independent from site type (21). α_{α} is the adsorption constant of the metal on site type

α . $H_0 = H(x=0)$ and $M_0 = M(x=0)$ are the free concentrations of protons and metal ions at distance $x = 0$ from the surface.

According to statistical mechanics, protons and the doubly positively charged metal ion in thermal equilibrium in an electric field originating from a surface with charge σ (C/m²) are distributed in such a way that their densities at distance x from the surface are given by

$$H(x) = H \exp\left(-\frac{F\psi(x)}{RT}\right) = H P(x), \quad (1.4)$$

$$M(x) = M \exp\left(-\frac{2F\psi(x)}{RT}\right) = M P^2(x), \quad (1.5)$$

where $\psi(x)$ (Volt = Joule/Coulomb) is the potential at distance x from the surface, F (96485 Coulomb/mol) is the Faraday-constant, R (8.314 J/(mol K)) is the molar gas constant, T (K) is the absolute temperature. The exponential term, called Boltzmann distribution, is abbreviated as $P(x)$. With Equations (1.4) and (1.5) and abbreviating $P(x=0)$ as P_0 , the three mass action laws involving four surface species ($X^\alpha\text{OH}_2$, $X^\alpha\text{OH}$, $X^\alpha\text{O}$, $X^\alpha\text{OM}$) are

$$X^\alpha\text{OH}_2 = k_1 X^\alpha\text{OH} H P_0, \quad (1.6)$$

$$X^\alpha\text{O} = k_2 X^\alpha\text{OH} \frac{1}{H P_0}, \quad (1.7)$$

$$X^\alpha\text{OM} = \alpha_\alpha X^\alpha\text{OH} \frac{M P_0}{H}. \quad (1.8)$$

Together with the site balance equation (11)

$$X_T^\alpha = X^\alpha\text{OH}_2 + X^\alpha\text{OH} + X^\alpha\text{O} + X^\alpha\text{OM}, \quad (\alpha = s, w) \quad (11)$$

we have four equations for four species, which can be combined to yield Equations (13) - (17):

$$X^{\alpha}OH_2(M, H) = X_T^{\alpha} \frac{k_1 P_0 H^2}{\delta_{\alpha}} \quad (13)$$

$$X^{\alpha}OH(M, H) = X_T^{\alpha} \frac{H}{\delta_{\alpha}} \quad (14)$$

$$X^{\alpha}O(M, H) = X_T^{\alpha} \frac{k_2/P_0}{\delta_{\alpha}} \quad (15)$$

$$X^{\alpha}OM(M, H) = X_T^{\alpha} \frac{\alpha_{\alpha} P_0 M}{\delta_{\alpha}} \quad (16)$$

where

$$\delta_{\alpha} = \alpha_{\alpha} P_0 M + H (1 + k_1 P_0 H) + \frac{k_2}{P_0} \quad (17)$$

We can express P_0 as a function of the other unknowns and the ion concentration in solution, c :

$$P_0(XOH_2, XO, XOM, c) = \exp\left(-\frac{F\psi_0(XOH_2, XO, XOM, c)}{RT}\right) \quad (I.9)$$

Proof: (1) We use our knowledge on the surface charge on each site type α

$$\sigma = \sigma^s + \sigma^w = XOH_2 - XO + XOM, \quad (I.10)$$

(2) The Gouy-Chapman theory gives the charge of an infinite plane immersed in an electrolyte composed of ions with charge $+ze$ and $-ze$ (e is the unit electronic charge) as a function of the potential:

$$\sigma = \sqrt{8 \cdot 10^3 RT \epsilon \epsilon_0 c} \sinh \frac{zF\psi_0}{2 RT}, \quad (I.11)$$

where c is the concentration of positive (or negative) ions, ϵ_0 the permittivity of free space ($8.854 \cdot 10^{-12} \text{ C}/(\text{Vm})$) and ϵ the dielectric constant of water (78.5). Using Equation (I.10) we calculate the potential at the surface $\psi_0 = \psi(x=0)$ by inverting the charge-potential relationship Equation (I.11):

$$\psi_0 = \frac{2 RT}{zF} \text{Arcsinh} \frac{\sigma^s + \sigma^w}{\sqrt{8 \cdot 10^3 RT \epsilon \epsilon_0 c}}. \quad (I.12)$$

(3) We use Equation (I.12) in the definition of the Boltzmann factor, which gives us (I.9).
q.e.d.

Equations (13) - (17) is a set of 8 equations: 4 equations for $\alpha = s$ and another 4 for $\alpha = w$. With Equation (I.9) it contains 10 unknowns, i.e. the 8 surface species concentrations and the 2 components concentrations, M and H . From this set the metal and proton isotherms

$$\underline{M}(M, H) = XOM, \quad (I.13)$$

$$\underline{H}(M, H) = XOH + 2 XOH_2 \quad (I.14)$$

can be calculated as functions of M and H . Because the surface species concentrations are given by a set of implicit equations of the type

$$X^\alpha OL_j (M, H) = f(M, H, X^{s,w} OL_m (M, H)) \quad (I.15)$$

where $X^{s,w} OL_m$ represents $X^\alpha OH_2$, $X^\alpha OH$, $X^\alpha O$, $X^\alpha OM$ with $\alpha = s, w$, the isotherms can usually be given only as numerical functions of M and H .

Appendix II: Proof of Analytical Solution of the Transport Equations

The adsorbed proton concentration \underline{H} is

$$\underline{H} = 2 \text{XOH}_2(\text{M}, \text{H}) + \text{XOH}(\text{M}, \text{H}) \quad (\text{II.1})$$

and the adsorbed metal concentration is

$$\underline{M} = \text{XOM}(\text{M}, \text{H}), \quad (\text{II.2})$$

thus

$$\underline{M} + \underline{H} = \text{XOM} + 2 \text{XOH}_2 + \text{XOH}, \quad (\text{II.3})$$

and with $\text{XOH}_2 = \text{XO}$ due to Equation (22)

$$\underline{M} + \underline{H} = \text{XOM} + \text{XOH}_2 + \text{XOH} + \text{XO} = \text{X}_T. \quad (\text{II.4})$$

We add Equations (7) and (8)

$$\left(\frac{q}{\phi} - \xi\right) \frac{d}{d\xi} (\underline{M} + \underline{H}_t) - \frac{\xi}{\phi} \frac{d}{d\xi} (\underline{M} + \underline{H}) = 0 \quad (\text{II.5})$$

and use the fact that the sum of the adsorbed metal and proton concentrations, Equation (II.4), is constant. The resulting differential equation is

$$\left(\frac{q}{\phi} - \xi\right) \frac{d}{d\xi} (M + H_t) = 0 \quad (II.6)$$

There are two solutions of Equation (II.6):

$$\frac{d}{d\xi} (M + H_t) = 0 \quad (II.7)$$

and

$$\xi = \frac{q}{\phi} \quad (II.8)$$

The solution Equation (II.8) is called non-retarded wave, the speed ξ of the wave being equal to the speed of the water q/ϕ . After using Equation (II.8) in Equation (I.3) we learn that the adsorbed metal concentration does not change across this non-retarded wave: $d/d\xi (XOM) = 0$ or

$$XOM(M, H) = XOM(M_+, H_+) \quad (II.9)$$

The adsorption isotherm (16) then fixes the relationship between M and H. Using the pristine water approximation Equation (22) for P in the isotherm, we get

$$XOM(M, H) = X_T \frac{\alpha \sqrt{\frac{k_2}{k_1}} \frac{M}{H^2}}{\alpha \sqrt{\frac{k_2}{k_1}} \frac{M}{H^2} + (1 + 2 \sqrt{k_1 k_2})} \quad (II.10)$$

This isotherm meets Equation (II.9) when

$$H = H_+ \sqrt{\frac{M}{M_+}} \quad (2\text{-wave, non-retarded}) \quad (II.11)$$

Whereas the non-retarded wave is determined by element independent properties Equation (24) of the oxide surface at low ionic strengths, the equation for the other wave -given by Equation (II.7)- involves only soluble species. Equation (II.7) states that the sum of the soluble concentrations is a conserved quantity, i.e. it does not change across the wave, $M + H_t = M_- + H_{t-}$, and using this together with the definition of H_t , Equation (9), we find

$$M = M_- - (H - H_-) - K_w \left(\frac{1}{H} - \frac{1}{H_-} \right) \quad (1\text{-wave, retarded}) \quad (II.12)$$

Appendix III: Retardation of the 1-Rarefaction Wave at Low Ionic Strength

The retardation of the 2-rarefaction wave follows from Equation (II.8) of Appendix II:

$$\rho_2 = \frac{q/\phi}{\xi_2} = 1 \quad (III.1)$$

The retardation of the 1-rarefaction wave can be calculated as follows:

Eliminating $q/(\phi\xi)$ in Equation (7) gives

$$\frac{q}{\phi \xi_1} = 1 + \frac{1}{\phi} \frac{\frac{dXOM(M, H)}{d\xi}}{\frac{dM}{d\xi}}, \quad (III.2)$$

where $\underline{M} = XOM = X^SOM + X^WOM$ was used. The derivatives with respect to ξ are directional derivatives along the 1-wave. When the function $M(H)$ given in Equation (25) is used to replace M in Equation (III.2), the directional derivative can be written as:

$$\frac{d}{d\xi} = \frac{d}{dH}, \quad (III.3)$$

and thus Equation (III.2) can be developed into the expression

$$\frac{q}{\phi \xi_1} = 1 + \frac{1}{\phi} \frac{\frac{dXOM(M, H)}{dH}}{\frac{dM}{dH}} = 1 + \frac{1}{\phi} \frac{\frac{\partial XOM(M, H)}{\partial M} \frac{dM(H)}{dH} + \frac{\partial XOM(M, H)}{\partial H} \frac{dH}{dH}}{\frac{dM(H)}{dH}} \quad (III.4)$$

which can be rewritten as

$$\frac{q}{\phi \xi_1} = 1 + \frac{1}{\phi} \frac{\partial XOM(M, H)}{\partial M} \left(1 + \frac{\frac{\partial XOM(M, H)}{\partial H} \frac{1}{\frac{dM(H)}{dH}}}{\frac{\partial XOM(M, H)}{\partial M}} \right) \quad (III.5)$$

Using the isotherms (16) with the P appropriate for low ionic strengths, i.e. Equation (22), the quotient of partial derivatives in Equation (III.5) becomes

$$\frac{\frac{\partial XOM(M, H)}{\partial H}}{\frac{\partial XOM(M, H)}{\partial M}} = -2 \frac{M}{H} \quad (III.6)$$

From Equation (25) we have

$$\frac{dM(H)}{dH} = - \left(1 + \frac{K_w}{H^2}\right) \quad (III.7)$$

Using Equations (III.6) and (III.7) in Equation (III.5), we find for the retardation

$$\rho_1 = \frac{q}{\phi \xi_1} = 1 + \frac{1}{\phi} \frac{\partial XOM(M, H)}{\partial M} \left(1 + \frac{2 \frac{M}{H}}{1 + \frac{K_w}{H^2}}\right) \quad (III.8)$$

Evaluation of $\partial XOM/\partial M$ with the isotherm (16) and the appropriate P from Equation (22) gives Equation (29) with Equation (30).

Appendix IV: The Jacobian of the Isotherms, the Retardation Matrix and its Eigenvectors

Because the adsorbed concentrations $\underline{M}(M, H)$ and $\underline{H}(M, H)$ depend only on the free concentrations M and H, the derivatives with respect to ξ can be written in the following way

$$\frac{d}{d\xi} = \frac{\partial}{\partial M} \frac{dM}{d\xi} + \frac{\partial}{\partial H} \frac{dH}{d\xi} \quad (IV.1)$$

Using Equation (IV.1) in Equations (7) and (8), dividing the resulting equations by ξ and re-writing them in matrix form leads to the eigenvalue problem

$$\underline{\mathbf{R}}(\mathbf{c}) \frac{d}{d\xi} \begin{Bmatrix} M \\ H_t \end{Bmatrix} = \rho(\mathbf{c}) \frac{d}{d\xi} \begin{Bmatrix} M \\ H_t \end{Bmatrix}, \quad (\text{IV.2})$$

where $\mathbf{c} = \{M, H\}$ is a point in concentration space.

The eigenvalue $\rho(\mathbf{c})$ is one of the values the quotient $q/(\phi \xi)$ can assume at point $\mathbf{c} = \{M, H\}$ in concentration space

$$\rho(\mathbf{c}) = \frac{q}{\phi \xi}. \quad (\text{IV.3})$$

The matrix $\underline{\mathbf{R}}(\mathbf{c})$, called retardation matrix, is

$$\underline{\mathbf{R}}(\mathbf{c}) = \underline{\mathbf{I}} + \frac{1}{\phi} \underline{\mathbf{Kd}}(\mathbf{c}) \begin{bmatrix} 1 & 0 \\ 0 & \frac{\partial H}{\partial H_t} \end{bmatrix}, \quad (\text{IV.4})$$

and the matrices $\underline{\mathbf{I}}$ and $\underline{\mathbf{Kd}}(\mathbf{c})$, the unit matrix and Jacobian of the isotherms, respectively, are

$$\underline{\mathbf{I}} = \begin{bmatrix} 1 & 0 \\ 0 & 1 \end{bmatrix},$$

$$\underline{\mathbf{Kd}}(\mathbf{c}) = \begin{bmatrix} \frac{\partial}{\partial M} \text{XOM}(\mathbf{c}) & \frac{\partial}{\partial H} \text{XOM}(\mathbf{c}) \\ \frac{\partial}{\partial M} (2\text{XOH}_2(\mathbf{c}) + \text{XOH}(\mathbf{c})) & \frac{\partial}{\partial H} (2\text{XOH}_2(\mathbf{c}) + \text{XOH}(\mathbf{c})) \end{bmatrix} \quad (\text{IV.5})$$

At any point $\mathbf{c} = \{M, H_t\}$ the retardation matrix, Equation (IV.4), has two eigenvalues $\rho_1(\mathbf{c})$ and $\rho_2(\mathbf{c})$. The system is non-degenerate, i.e.

$$\rho_1(\mathbf{c}) > \rho_2(\mathbf{c}) \geq 1. \quad (\text{IV.6})$$

For low ionic strengths, i.e. $I \leq 10^{-4} \text{ M}$, we can use approximation (22) for P. Then

$$\underline{\mathbf{Kd}}(\mathbf{c}) = \begin{bmatrix} \frac{\partial}{\partial M} \text{XOM}(\mathbf{c}) & \frac{\partial}{\partial H} \text{XOM}(\mathbf{c}) \\ \frac{\partial}{\partial M} (2\text{XOH}_2(\mathbf{c}) + \text{XOH}(\mathbf{c})) & \frac{\partial}{\partial H} (2\text{XOH}_2(\mathbf{c}) + \text{XOH}(\mathbf{c})) \end{bmatrix} = \frac{\partial \text{XOM}(\mathbf{c})}{\partial M} \begin{bmatrix} 1 & -\frac{2M}{H} \\ -1 & \frac{2M}{H} \end{bmatrix} \quad (\text{IV.7})$$

with

$$\frac{\partial \text{XOM}(\mathbf{c})}{\partial M} = X_T \frac{\alpha \text{PZC} (1 + 2 k_1 \text{PZC}) H^2}{(\alpha \text{PZC} M + H^2 (1 + 2 k_1 \text{PZC}))^2} \quad (\text{IV.8})$$

The eigenvalues of $\underline{\mathbf{Kd}}$ are then

$$\{kd_1, kd_2\} = \frac{\partial \text{XOM}[\mathbf{c}]}{\partial M} \left\{ \frac{H + 2M}{H}, 0 \right\} \quad (\text{IV.9})$$

Because

$$\frac{dH}{dH_t} = \frac{1}{1 + \frac{K_w}{H^2}} \quad (\text{IV.10})$$

the eigenvalues are

$$\rho_1(\mathbf{c}) = 1 + \frac{1}{\phi} \frac{\partial \text{XOM}(\mathbf{c})}{\partial M} \left(1 + \frac{2HM}{H^2 + K_w}\right), \quad (\text{IV.11})$$

$$\rho_2(\mathbf{c}) = 1, \quad (\text{IV.12})$$

which is consistent with Equations (29) and (30).

To each eigenvalue ρ_i of the retardation matrix belongs a right eigenvector (see Equation (IV.2))

$$\mathbf{r}_k = \kappa \frac{d}{d\xi} \begin{Bmatrix} M \\ H_t \end{Bmatrix}. \quad (\text{IV.13})$$

This means that two infinitesimally separated positions \mathbf{c} and $\mathbf{c} + d\mathbf{c}$ on the k-wave are connected by a vector pointing in the direction of the (right) eigenvector \mathbf{r}_k

$$\frac{d}{d\xi} \mathbf{c} = \frac{d}{d\xi} \begin{Bmatrix} M \\ H_t \end{Bmatrix} = \kappa \mathbf{r}(\mathbf{c}). \quad (\text{IV.14})$$

We take $\kappa = 1$ and choose the direction of the k-eigenvector such that the retardation $\rho_k(\mathbf{c})$ of the k-wave decreases in the direction of the k-eigenvector

$$(\text{grad } \rho_k, \mathbf{r}_k) < 0. \quad (\text{IV.15})$$

Let $\mathbf{c}(k, n)$ be the k-wave in concentration space, with n being an index denoting successive points on the wave. We can construct a k-wave $\mathbf{c}(k, n)$ by integrating Equation (IV.14), i.e. compose the wave out of piecewise

straight segments. The fastest integration procedure would be the Euler method

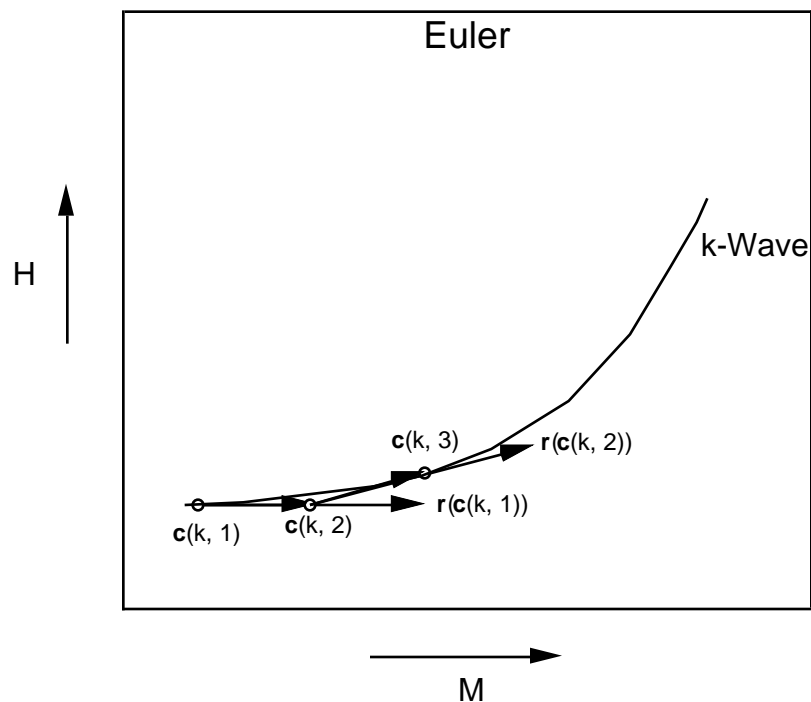
$$\mathbf{c}(k, n) = \mathbf{c}(k, n-1) + \delta \mathbf{r}_k(\mathbf{c}(k, n-1)), \quad (\text{IV.16})$$

where δ is the length of the segments pointing in the direction of the eigenvector $\mathbf{r}_k(\mathbf{c}(k, n-1))$ at the beginning of the segment ($\mathbf{c}(k, n-1)$).

Runge-Kutta methods are more accurate, because they use an averaged direction $\mathbf{step}(\mathbf{c}(k, n-1))$ instead of the direction $\mathbf{r}_k(\mathbf{c}(k, n-1))$:

$$\mathbf{c}(k, n) = \mathbf{c}(k, n-1) + \delta \mathbf{step}(\mathbf{c}(k, n-1)), \quad (\text{IV.17})$$

where in this paper we used the following averaging method



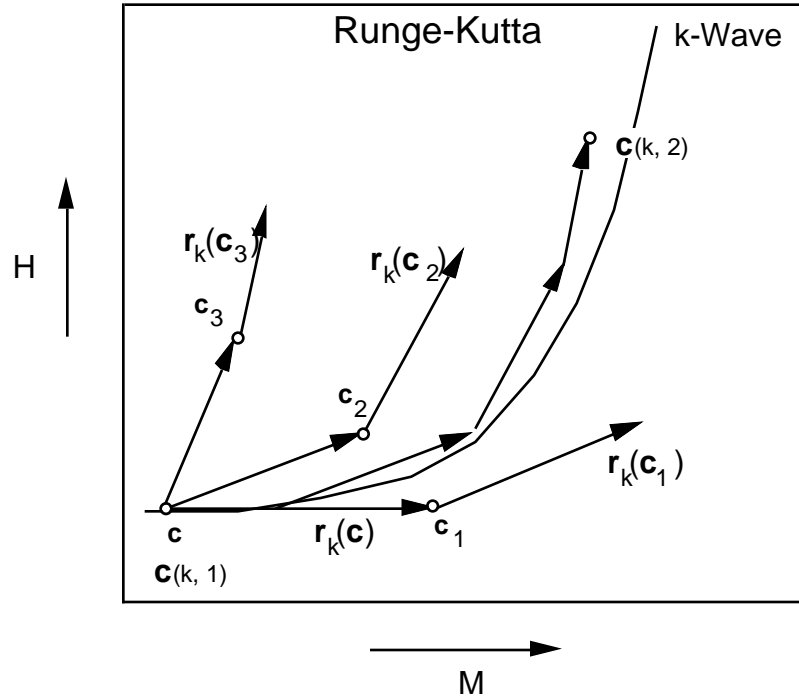


Figure IV.1: Euler and Runge-Kutta integration method for transport equations (IV.14). The k-wave is composed of line segments of length δ pointing in the direction of the eigenvector evaluated at the start of the segment.

$$\mathbf{step}(\mathbf{c}) = \frac{1}{6} \mathbf{r}_k(\mathbf{c}) + 2 \mathbf{r}_k(\mathbf{c}_1) + \mathbf{r}_k(\mathbf{c}_2) + 2 \mathbf{r}_k(\mathbf{c}_3) \quad (\text{IV.18})$$

$$\mathbf{c}_1 = \mathbf{c} + \frac{\delta}{2} \mathbf{r}_k(\mathbf{c}), \quad \mathbf{c}_2 = \mathbf{c} + \frac{\delta}{2} \mathbf{r}_k(\mathbf{c}_1), \quad \mathbf{c}_3 = \mathbf{c} + \delta \mathbf{r}_k(\mathbf{c}_2) \quad (\text{IV.19})$$

Figure IV.1 depicts the Euler and Runge-Kutta methods Equations (IV.16) - (IV.19).

Appendix V: Computation of the 2-Shock

Solving Equations (3) and (4) for the shock-retardation σ

$$\sigma = 1 + \frac{q/\phi}{\Delta x/\Delta t}, \quad (\text{V.1})$$

gives the so-called Rankine Hugoniot relation:

$$\sigma = 1 + \frac{1}{\phi} \frac{\Delta \underline{M}}{\Delta M} = 1 + \frac{1}{\phi} \frac{\Delta \underline{H}}{\Delta H_t}, \quad (\text{V.2})$$

where Δ denotes the concentration jump across the shock. For the 2-shock (see Figures 1 and 2, subscript m is omitted for brevity),

$$\begin{aligned} \Delta M &= M - M_+, \\ \Delta H_t &= H_t - H_{t+}, \\ \Delta \underline{M} &= \underline{M}(M, H) - \underline{M}(M_+, H_+), \\ \Delta \underline{H} &= \underline{H}(M, H) - \underline{H}(M_+, H_+). \end{aligned} \quad (\text{V.3})$$

The first of the two equations (V.2) is similar to Equation (III.2), derived for rarefaction waves, as can be seen replacing \underline{M} with XOM . Replacing also \underline{H} with $XOH + 2 XOH_2$ changes Equation (V.2) into

$$\frac{\Delta XOM(M, H)}{\Delta M} = \frac{\Delta (XOH(M, H) + 2 XOH_2(M, H))}{\Delta H_t} \quad (\text{V.4})$$

which is called integral coherence condition in chromatography [Helfferrich and Klein, 1970].

Equation (V.4) with Equation (V.3) can be solved for M as a function of H . The Lax entropy condition [Lax, 1957]

$$\sigma_2 < \rho_1(M_m, H_m) \tag{V.5}$$

selects from the solutions the one, $M(M_+, H_+, H)$, that has physical meaning in that it is faster than the 1-rarefaction wave behind it. It is the 2-shock.

Version: 26 April 2015